



CONFIDENTIAL

Copy
RM L56J25

NACA RM L56J25

UNCLASSIFIED

C.1



RESEARCH MEMORANDUM

INVESTIGATION AT HIGH SUBSONIC SPEEDS OF
THE EFFECTS OF VARIOUS HORIZONTAL FUSELAGE FOREBODY
FINS ON THE DIRECTIONAL AND LONGITUDINAL STABILITY
OF A COMPLETE MODEL HAVING

A 45° SWEEPBACK WING

By William C. Sleeman, Jr. ✓

Langley Aeronautical Laboratory
Langley Field, Va.

LIBRARY COPY

JAN 29 1957

LANGLEY AERONAUTICAL LABORATORY
LIBRARY NACA
LANGLEY FIELD, VIRGINIA

CLASSIFIED DOCUMENT

This material contains information affecting the National Defense of the United States within the meaning of the espionage laws, Title 18, U.S.C., Secs. 793 and 794, the transmission or revelation of which in any manner to an unauthorized person is prohibited by law.

NATIONAL ADVISORY COMMITTEE FOR AERONAUTICS

WASHINGTON
January 16, 1957

CLASSIFICATION CHANGED

UNCLASSIFIED

By authority of *AM #17* *3/18/64* *W.S.M.*

CONFIDENTIAL

UNCLASSIFIED

NATIONAL ADVISORY COMMITTEE FOR AERONAUTICS

RESEARCH MEMORANDUM

INVESTIGATION AT HIGH SUBSONIC SPEEDS OF
THE EFFECTS OF VARIOUS HORIZONTAL FUSELAGE FOREBODY
FINS ON THE DIRECTIONAL AND LONGITUDINAL STABILITY
OF A COMPLETE MODEL HAVING
A 45° SWEEPBACK WING
By William C. Sleeman, Jr.

SUMMARY

An investigation has been conducted in the Langley high-speed 7- by 10-foot tunnel of the effects of various horizontal fuselage forebody fins on the directional and longitudinal stability characteristics at high subsonic speeds of a complete model having a 45° swept-back wing mounted in a high position on the fuselage. The model wing had an aspect ratio of 4, a taper ratio of 0.30, and NACA 65A006 airfoil sections parallel to the free stream. The Mach number range for most of the tests extended from 0.60 to 0.92 and the angle-of-attack range was from -2° to 24° at the lowest test Mach number.

The basic model of this investigation became directionally unstable at high angles of attack and generally small or insignificant gains in directional stability were realized by addition of a pair of rectangular canard-type fins in several locations on the sides of the fuselage nose. Long and narrow strakes on the sides of the fuselage nose were, however, found to be effective in increasing the directional stability of the model throughout the moderate and high angle-of-attack range. The favorable effect of the largest strakes tested caused the tail-off configuration to become directionally stable at moderately high angles of attack and there is evidence that this effect was predominant on the forward portion of the model rather than over the fuselage afterbody. Although the increment in tail contribution to directional stability due to the large strakes was unfavorable, the beneficial effect of the wing-fuselage characteristics was so large that the complete-model stability was greater with the large strakes on than without. The most effective strakes produced appreciable destabilizing pitching moments at moderate and high angles of attack; however, these unfavorable pitching moments

could be reduced by decreasing the strake size. The smallest strakes gave pitching-moment results which were not appreciably different from the satisfactory basic-model variation and still provided some increases in directional stability.

INTRODUCTION

The problem of maintaining directional stability throughout a reasonably large angle-of-attack range has received much recent attention because many current airplane configurations have been found deficient in this respect. A number of wind-tunnel investigations have dealt with the effects of various design parameters on airplane directional stability at high angles of attack (for example see refs. 1 to 3), and the importance of the vortex flow from the fuselage nose has been indicated with regard to the fuselage and vertical-tail contribution to stability. A means for improving the directional stability characteristics at high angles of attack through possible alteration of the flow from the fuselage nose was found in connection with a spin-recovery study of a swept-wing model reported in reference 4. These tests demonstrated that significant improvement in model flight behavior at high angles of attack could be gained by use of canard fins projecting from the fuselage sides. Low-speed wind-tunnel force measurements on a configuration similar to that of reference 4 are given in reference 5.

The present investigation was undertaken to determine whether improvements in directional stability at high angles of attack and at high subsonic speeds could be made by use of small canard fins. The present tests were conducted with the high-wing circular-fuselage model of references 1 and 2 which had a 45° sweptback wing of aspect ratio 4. Rectangular fins having an exposed aspect ratio of approximately 0.60 were tested in various longitudinal positions on the sides of the fuselage nose and effects of fin incidence and dihedral were studied. In addition to the rectangular fins, several very long and narrow strakes were studied in one location on the sides of the fuselage. The test Mach number range extended from 0.60 to 0.92 for most of the tests and the angle-of-attack range extended from -2° to 24° at the lowest test Mach number.

SYMBOLS

The lateral stability results of this investigation are referred to the body axis system shown in figure 1 and the longitudinal characteristics in pitch are referred to the stability axes. Moment coefficients

are given about a moment reference point located on the fuselage center line at a longitudinal position corresponding to the quarter chord of the wing mean aerodynamic chord.

C_L	lift coefficient, $Lift/qS$
C_D	drag coefficient, $Drag/qS$
C_m	pitching-moment coefficient, $\frac{\text{Pitching moment}}{qS\bar{c}}$
C_l	rolling-moment coefficient, $\frac{\text{Rolling moment}}{qSb}$
C_n	yawing-moment coefficient, $\frac{\text{Yawing moment}}{qSb}$
C_y	lateral-force coefficient, $\frac{\text{Lateral force}}{qS}$
b	wing span, ft
\bar{c}	wing mean aerodynamic chord, ft
M	Mach number
q	dynamic pressure, $\frac{\rho V^2}{2}$, lb/sq ft
S	wing area, sq ft
V	free-stream velocity, ft/sec
i_f	fin incidence, positive leading edge up, deg
α	angle of attack of fuselage center line, deg
β	angle of sideslip, deg
Γ	dihedral angle of fin, deg (see fig. 3)
ρ	air density, slugs/cu ft

Subscripts:

β denotes partial derivative of a coefficient with respect to sideslip, for example, $C_{L\beta} = \frac{\partial C_L}{\partial \beta}$

t denotes increment due to addition of tail surfaces

Configuration designation:

W wing

F fuselage

V vertical tail

H horizontal tail

f_1, f_2, \dots, f_8 fin configuration (see fig. 3)

MODEL DESCRIPTION

The basic model configuration used in this investigation is shown in figure 2. The aspect-ratio-4 wing was swept back 45° at the quarter chord, had a taper ratio of 0.3, and had NACA 65A006 airfoil sections parallel to the free-stream direction. The wing was constructed of 2024S-T aluminum and was mounted 11.1-percent wing semispan above the fuselage center line. The vertical tail which was swept back 28° had NACA 63A009 airfoil sections streamwise and the 45° sweptback horizontal tail had NACA 65A006 airfoil sections parallel to the free-stream direction.

The various fin arrangements investigated are shown in figure 3. The fins were constructed from 1/32-inch-thick brass and were mounted rigidly to the fuselage, any spaces existing between the fin root and fuselage being filled with a sealer to prevent air flow through the gap. The exposed aspect ratio of the rectangular fin was 0.60. With the exception of fin f_2 , all the fins were tested in pairs mounted on the fuselage sides at a height corresponding to the fuselage center line. Fin f_2 was tested singularly and was mounted on top of the fuselage. Effects of fin dihedral were studied with fin f_3 as shown in figure 3.

A different approach was followed in attempting to achieve an effective fin configuration by testing the very slender horizontal

fuselage forebody strakes f_6 to f_8 . The size of fin f_6 was halved by decreasing the width to obtain fin f_7 . The rear half of fin f_7 was removed to obtain fin f_8 .

TESTS AND CORRECTIONS

Tests

The present investigation was conducted in the Langley high-speed 7- by 10-foot tunnel over a Mach number range from 0.60 to 0.85 for all configurations and was extended to a Mach number of 0.92 for some configurations. The average test Reynolds number based on the wing mean aerodynamic chord was approximately 3×10^6 for these test conditions.

The model was mounted on a six-component internal strain-gage balance which was supported by a variable-angle sting. The lateral stability derivatives of this investigation were obtained from tests conducted through the angle-of-attack range with the model at fixed sideslip angles of $\pm 4^\circ$. Longitudinal stability characteristics were investigated at 0° sideslip and some limited tests through the sideslip range were made at constant angles of attack. The maximum angle-of-attack range covered extended from approximately -2° to 24° and the sideslip angles varied from -4° to 12° for the variable sideslip tests.

Corrections

Jet-boundary corrections to the angles of attack and drag coefficients determined from reference 6 were added to the data. Blockage corrections applied to the Mach number and dynamic pressure were determined from reference 7. Drag coefficients have been corrected for a tunnel buoyancy effect and corrections have been applied such that the base pressure conditions correspond to free-stream static pressure. The model angles of attack and sideslip have been corrected for deflection of the balance and sting support under load.

RESULTS AND DISCUSSION

Presentation of Results

Lateral stability derivatives of the model with the various fin configurations are presented in figures 4 to 6 and aerodynamic characteristics in sideslip for the model with fin f_6 are given in figure 7.

Aerodynamic characteristics in pitch for the basic model and for the model with the strakes installed are presented in figures 8 to 10. A summary of the most pertinent fin effects is presented in figures 11 and 12. It should be pointed out that, in general, the results obtained at the lowest test Mach number indicated the trends obtained at the higher Mach numbers; consequently, in some cases, data are presented only for $M = 0.60$ where the maximum test angle-of-attack range was covered.

Discussion

Lateral stability of basic model and with rectangular fins.- The lateral stability derivatives for the basic model presented in figure 4 show a large reduction in the directional stability $C_{n\beta}$ as the angle of attack increased beyond approximately 10° . For angles of attack above about 18° at a Mach number of 0.60, an increasing directional instability was indicated with increasing angle of attack. This increase in instability is due to some extent to the wing-fuselage behavior; however, most of it can probably be attributed to decreases in the vertical-tail contribution. (See figs. 12(a) and 12(c).)

The various rectangular-fin configurations tested were studied in attempts either to eliminate the occurrence of directional instability or to effect a significant delay in the angle of attack at which the instability occurred. The results presented in figure 4 indicate that the rectangular-fin arrangements tested had no appreciable favorable effect on the directional stability characteristics of the model.

Lateral stability of model with forebody strakes.- Inasmuch as the fairly wide range of fin positions studied effected only minor directional stability gains with the fairly large rectangular fins, a slightly different approach was taken in testing the strakes extending along the entire fuselage nose. Directional stability characteristics of the model with the strakes are summarized in figure 11 for a Mach number of 0.60. These results show that substantial gains in the directional stability of the basic configuration were realized by addition of the large strakes (fin f_6) for angles of attack greater than about 9° . The angle of attack at which the directional stability started to decrease was increased from approximately 9° for the basic model to about 14° for the model with fin f_6 and the occurrence of directional instability was delayed from approximately 18° to an angle of attack of 22° by use of the large strakes.

A fairly substantial reduction in directional stability benefits of fin f_6 was encountered in reducing the area of fin f_6 in half to form fin f_7 . When the rear half of fin f_7 was removed to form fin f_8 , the

directional stability characteristics of the model were essentially the same as those obtained with fin f_7 (fig. 11).

Longitudinal stability of model with the forebody strakes.- The use of horizontal fins located ahead of the center of gravity would be expected to have an adverse effect on longitudinal stability and the extent of this effect for the present model is shown in the right-hand portion of figure 11. The pitching-moment variation with angle of attack for the basic model is considered to be satisfactory whereas the pitching-moment characteristics of the model with fin f_6 show a highly undesirable pitch-up tendency over a wide range of angles of attack. The smaller strakes, fins f_7 and f_8 , were tested in order to determine the extent to which the adverse effects of fin f_6 on longitudinal stability could be minimized and still retain an effective arrangement from the standpoint of directional stability characteristics. The results presented in figure 11 show that appreciable reductions in adverse longitudinal characteristics accompanied reductions in the size of fin f_6 and the pitching-moment characteristics with the smallest fin f_8 were not markedly inferior to the basic model. Of course, as mentioned previously, the smallest strakes, which gave minimum pitching-moment changes were much less effective in increasing directional stability at high angles than the largest strakes.

Characteristics in sideslip with the large forebody strakes.- Additional test results were obtained with fin f_6 to determine the directional stability characteristics for sideslip angles up to approximately 12° and these results are presented in figure 7. These data show no appreciable nonlinearities in yawing moments for the conditions tested and therefore the directional stability parameters obtained from tests at $\pm 4^\circ$ sideslip would be expected to indicate fin effects to at least an angle of sideslip of 10° and an angle of attack of 16° . Data for the basic model configuration in sideslip were obtained from reference 2 inasmuch as sideslip tests of the fin-removed configuration were not made in the present investigation. Yawing-moment data at $M = 0.80$ obtained from reference 2 and transferred to the body-axis system are presented in figure 12(b) to show the effect of fin f_6 through the sideslip range. This comparison shows that the large strakes were effective in providing a stabilizing yawing-moment contribution throughout the test sideslip-angle range at approximately an angle of attack of 16° .

Effect of large forebody strakes with and without tail surfaces.- Additional information relating to the effectiveness of fin f_6 is given in figure 12(a) which shows the fin effectiveness with and without the tail surfaces. Tail-off results without the fin were obtained from reference 2 and transferred to the body-axis system of the present data. Directional stability characteristics show a large favorable effect of

the strakes at high angles of attack for the wing fuselage whereas the tail contribution (fig. 12(c)) at high angles was less with the strakes on than for the basic model. Even though the increment in tail contribution due to the strakes was unfavorable, the beneficial effect on the wing-fuselage characteristics was so large that the complete-model stability was greater with the strakes on than without the strakes. Some insight into the favorable effect of the strakes on the wing-fuselage characteristics may be gained from a comparison of lateral-force derivatives with and without fin f_{ζ} presented in figure 12(a). For angles of attack above 11° the strakes contributed a positive increment of $C_{Y_{\beta}}$ with increases in angle of attack (fig. 12(a)) and at the highest test angles of attack ($M = 0.60$, fig. 5) positive values of $C_{Y_{\beta}}$ were indicated for the wing-fuselage configuration with fin f_{ζ} . Directional stability characteristics presented in figure 12(a) also show a large positive increment of $C_{N_{\beta}}$ due to the strakes and at high angles of attack the tail-off configuration became directionally stable. This occurrence of positive increments in both $C_{Y_{\beta}}$ and $C_{N_{\beta}}$ due to the strakes for the tail-off configuration indicates that the effective center of pressure of the incremental load due to the strakes was ahead of the reference center of moments. It appears furthermore that stabilizing (positive $C_{N_{\beta}}$) flow-angularity effects on the fuselage afterbody would not be expected to occur for the tail-off configuration in conjunction with positive incremental values of $C_{Y_{\beta}}$. On the other hand, the destabilizing effect of the strakes on the tail contribution at high angles (fig. 12(a)) is consistent with positive increments in $C_{Y_{\beta}}$ due to the strakes with the tail on. It therefore appears that the favorable contribution of the strakes to directional stability of the model were associated with effects on the forebody of the wing-fuselage configuration. The extent to which this effect occurs on the fuselage nose and on the wing is not known; however, rather large effects of the strakes on the effective dihedral parameter $C_{l_{\beta}}$ did occur (see figs. 4 and 5). Inasmuch as the strake moment arm in roll was very small, the large magnitude of the positive increments of $C_{l_{\beta}}$ due to the strakes at high angles of attack suggest that the strakes had a significant indirect effect on the wing contribution to rolling moments.

CONCLUSIONS

The results of an investigation conducted in the Langley high-speed 7-foot tunnel to study the effects of various fuselage forebody

fins on the directional and longitudinal stability at high angles of attack of a high wing model indicated the following conclusions:

1. The directional instability for the basic model which occurred at moderately high angles of attack was not appreciably alleviated by use of a pair of rectangular fins located at various positions on the fuselage nose.

2. Long and narrow horizontal strakes on the sides of the fuselage nose were found to be effective in increasing the directional stability of the model throughout the moderate and high angle-of-attack range. This favorable effect for the largest strakes tested caused the tail-off configuration to become directionally stable at moderately high angles of attack and there is evidence that this effect was predominant on the forward sections of the model rather than over the fuselage afterbody.

3. Although the increment in tail contribution to directional stability due to the large strakes was unfavorable, the beneficial effect of the wing-fuselage characteristics was so large that the complete-model stability was greater with the large strakes on than without. The angle-of-attack range over which the basic model was directionally stable was extended by addition of the strakes; however, directional instability occurred at the highest test angles both with and without the strakes.

4. The most effective strakes produced appreciable destabilizing pitching moments at moderate and high angles of attack; however, these unfavorable pitching moments could be reduced by decreasing the strake size. Installation of the smallest strakes gave pitching-moment results which were not appreciably different from the satisfactory basic-model characteristics and still provided some increases in directional stability.

Langley Aeronautical Laboratory,
National Advisory Committee for Aeronautics,
Langley Field, Va., October 10, 1956.

REFERENCES

1. King, Thomas J., Jr.: Wind-Tunnel Investigation at High Subsonic Speeds of Some Effects of Fuselage Cross-Section Shape and Wing Height on the Static Longitudinal and Lateral Stability Characteristics of a Model Having a 45° Swept Wing. NACA RM L55J25, 1956.
2. Silvers, H. Norman, and King, Thomas J., Jr.: Investigation at High Subsonic Speeds of the Effect of Horizontal-Tail Location on Longitudinal and Lateral Stability Characteristics of a Complete Model Having a Sweptback Wing in a High Location. NACA RM L56B10, 1956.
3. Polhamus, Edward C., and Hallissy, Joseph M., Jr.: Effect of Airplane Configuration on Static Stability at Subsonic and Transonic Speeds. NACA RM L56A09a, 1956.
4. Klinar, Walter J.: A Study by Means of a Dynamic-Model Investigation of the Use of Canard Surfaces As an Aid in Recovering From Spins and as a Means for Preventing Directional Divergence Near the Stall. NACA RM L56B23, 1956.
5. Paulson, John W., and Boisseau, Peter C.: Low-Speed Investigation of the Effect of Small Canard Surfaces on the Directional Stability of a Sweptback-Wing Fighter-Airplane Model. NACA RM L56F19a, 1956.
6. Gillis, Clarence L., Polhamus, Edward C., and Gray, Joseph L., Jr.: Charts for Determining Jet-Boundary Corrections for Complete Models in the 7- by 10-Foot Closed Rectangular Wind Tunnels. NACA WR L-123, 1945. (Formerly NACA ARR L5G31.)
7. Herriot, John G.: Blockage Corrections for Three-Dimensional-Flow Closed-Throat Wind Tunnels, With Consideration of the Effect of Compressibility. NACA Rep. 995, 1950. (Supersedes NACA RM A7B28.)

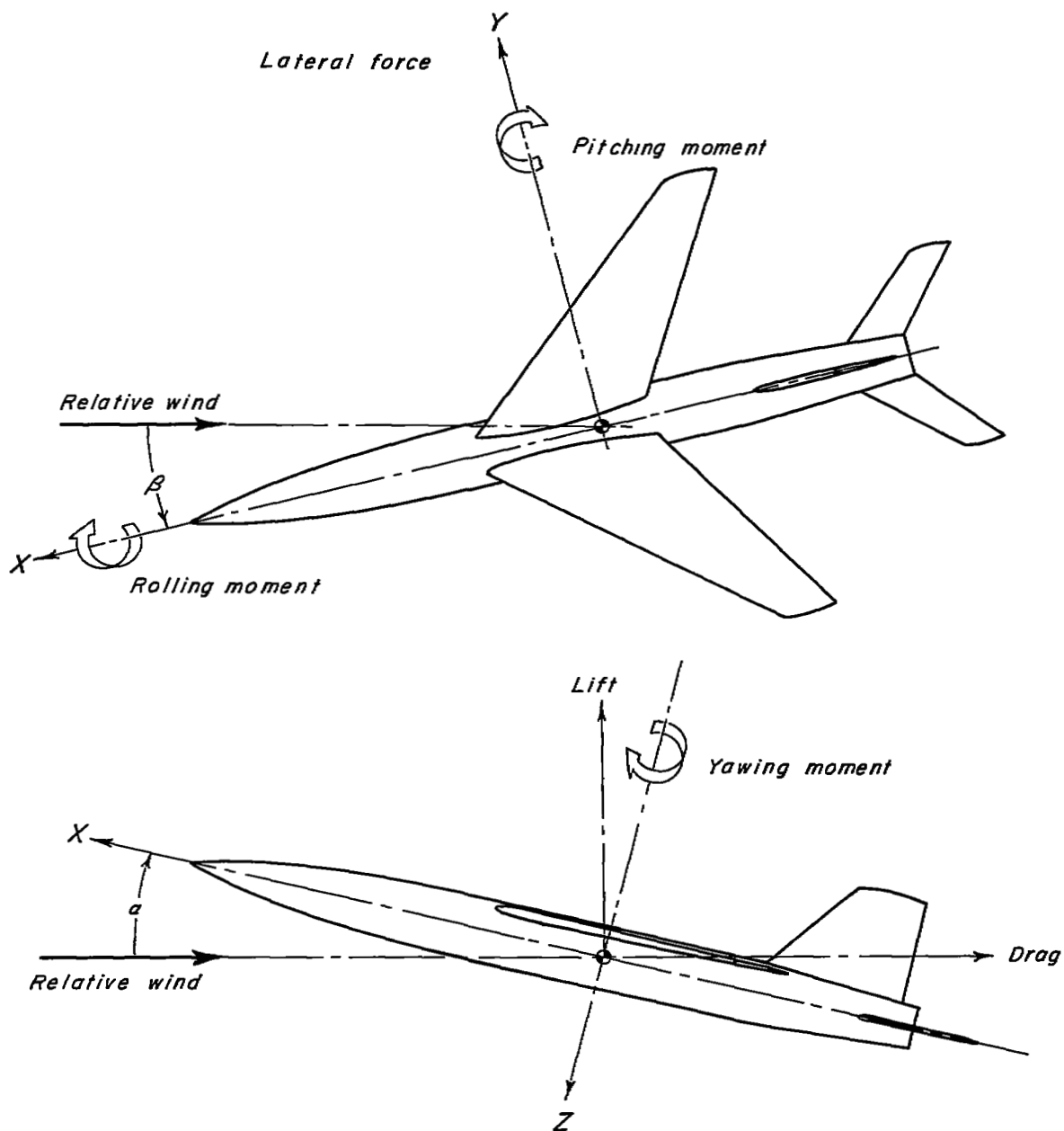


Figure 1.- Body reference axes showing positive directions of forces, moments, and angular deflections.

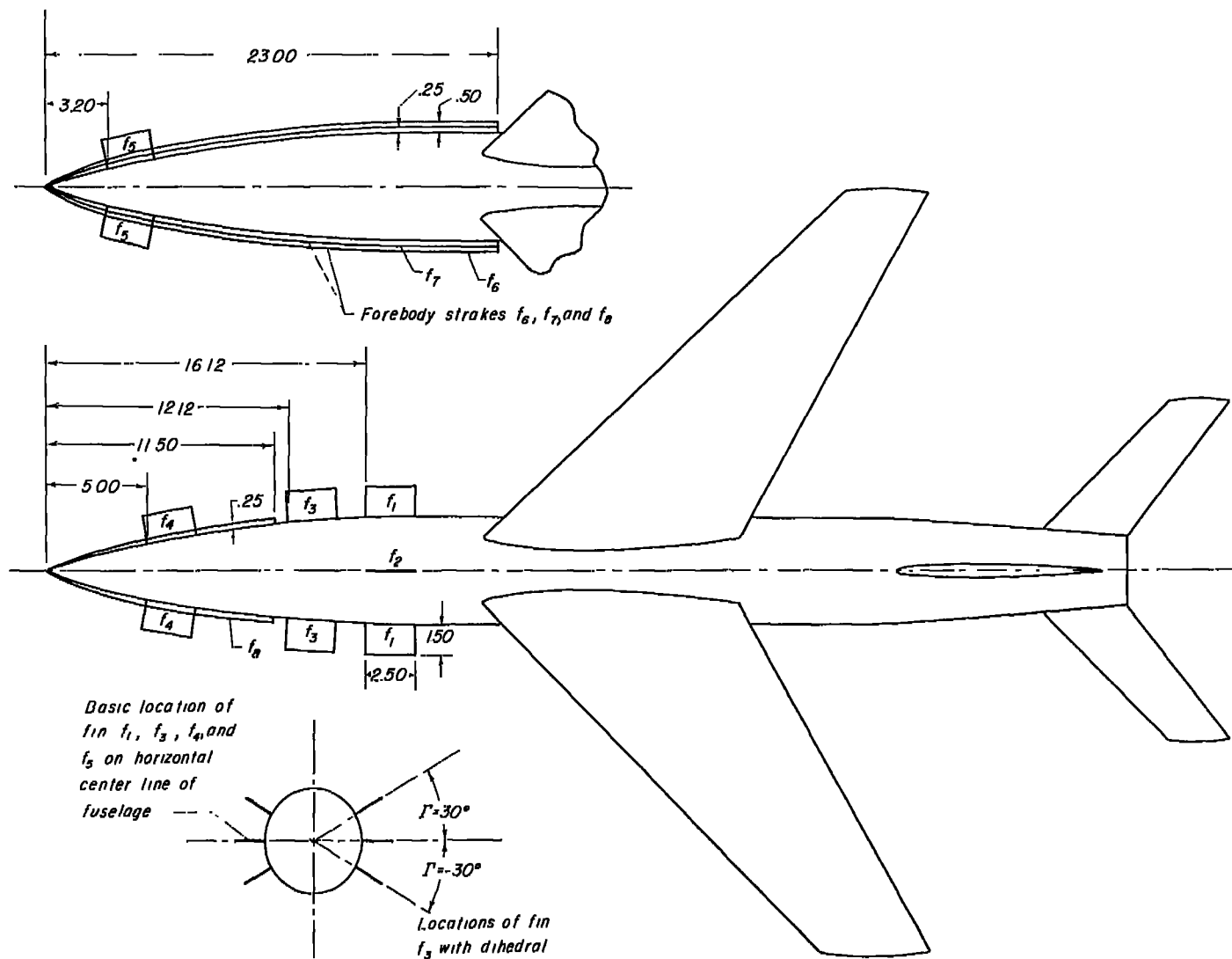


Figure 3.- Sketch of the various fin arrangements tested and showing the locations tested on the model. Linear dimensions are in inches.

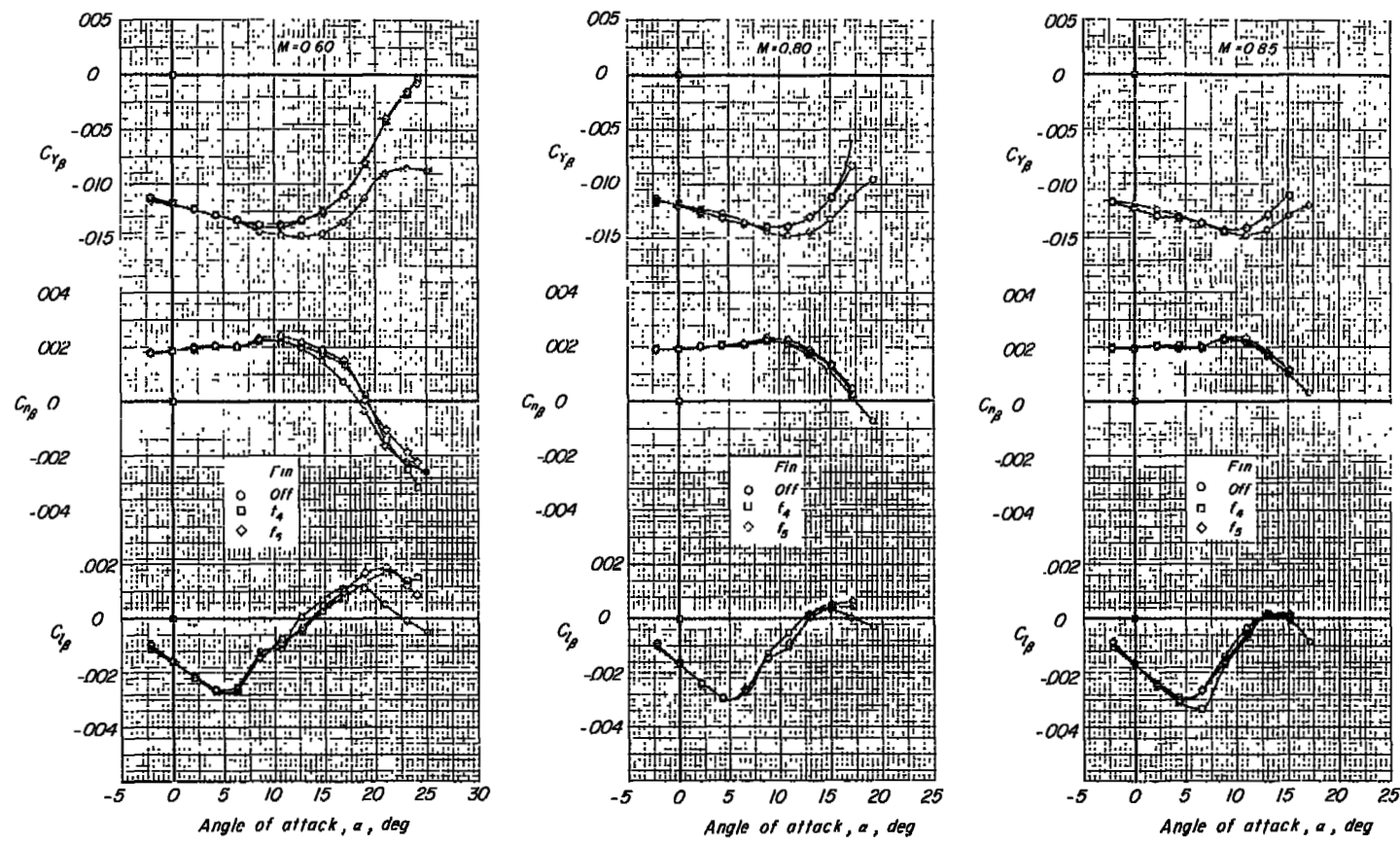


Figure 4.- Lateral stability derivatives of the basic model and the model with various rectangular fin configurations.

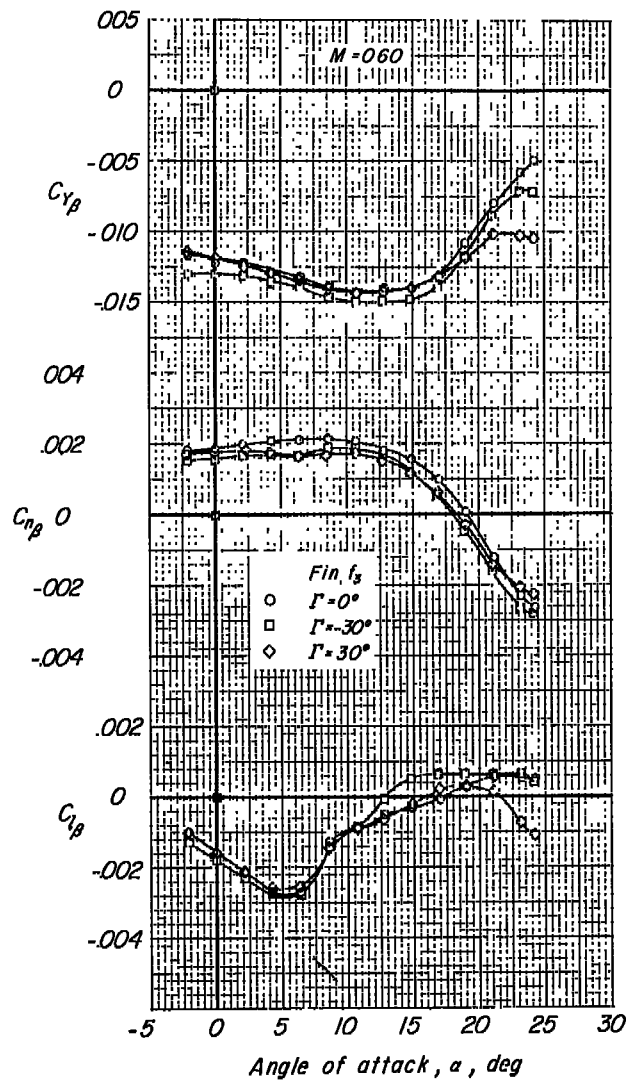
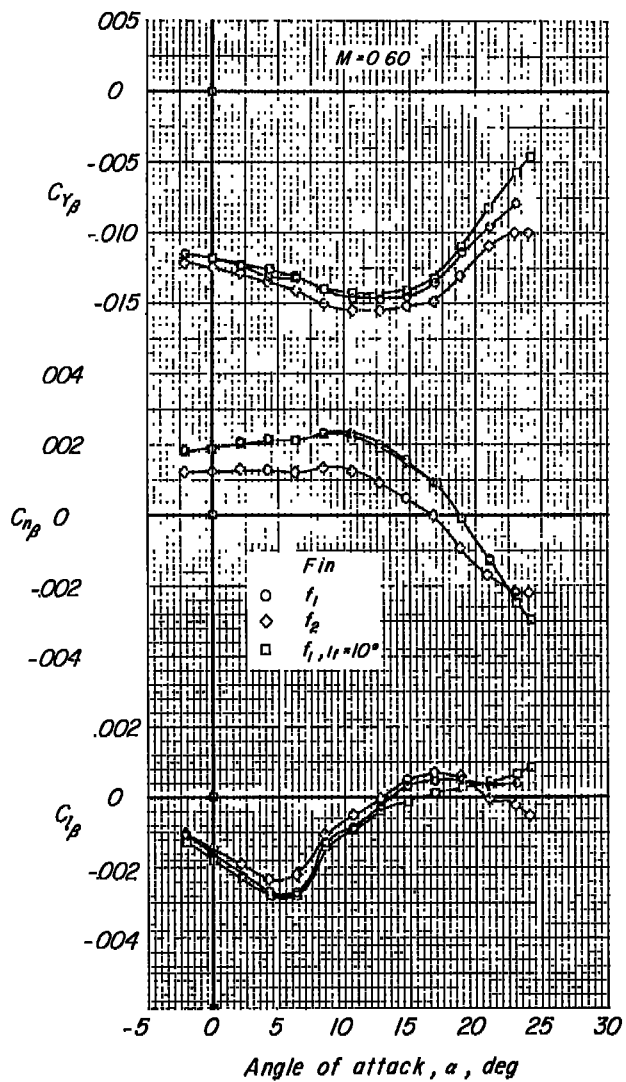


Figure 4.- Concluded.

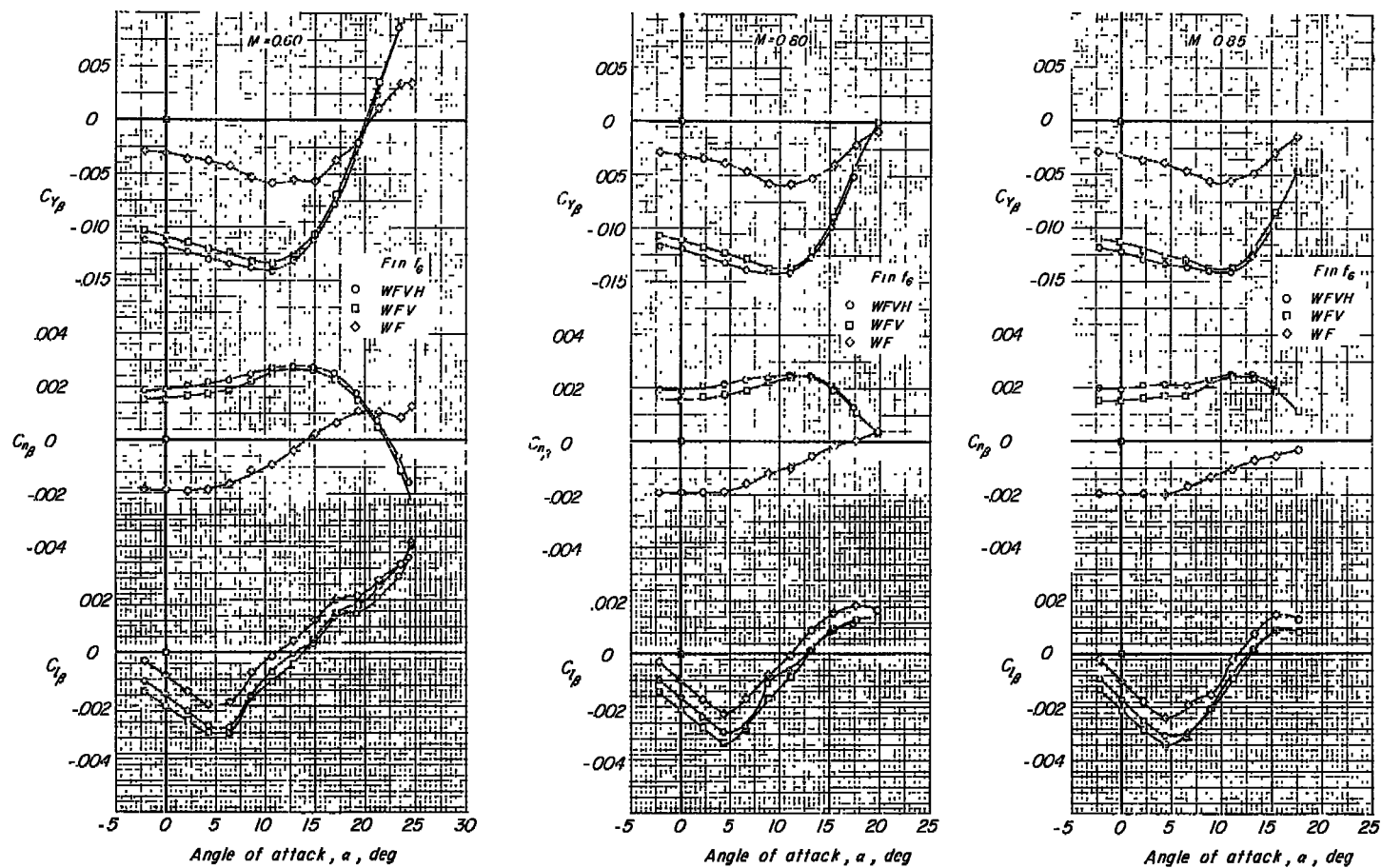


Figure 5.- Lateral stability derivatives of the model with the large strakes, fin f_6 , showing effects of addition of the tail surfaces.

Fin f_6

○ WFVH

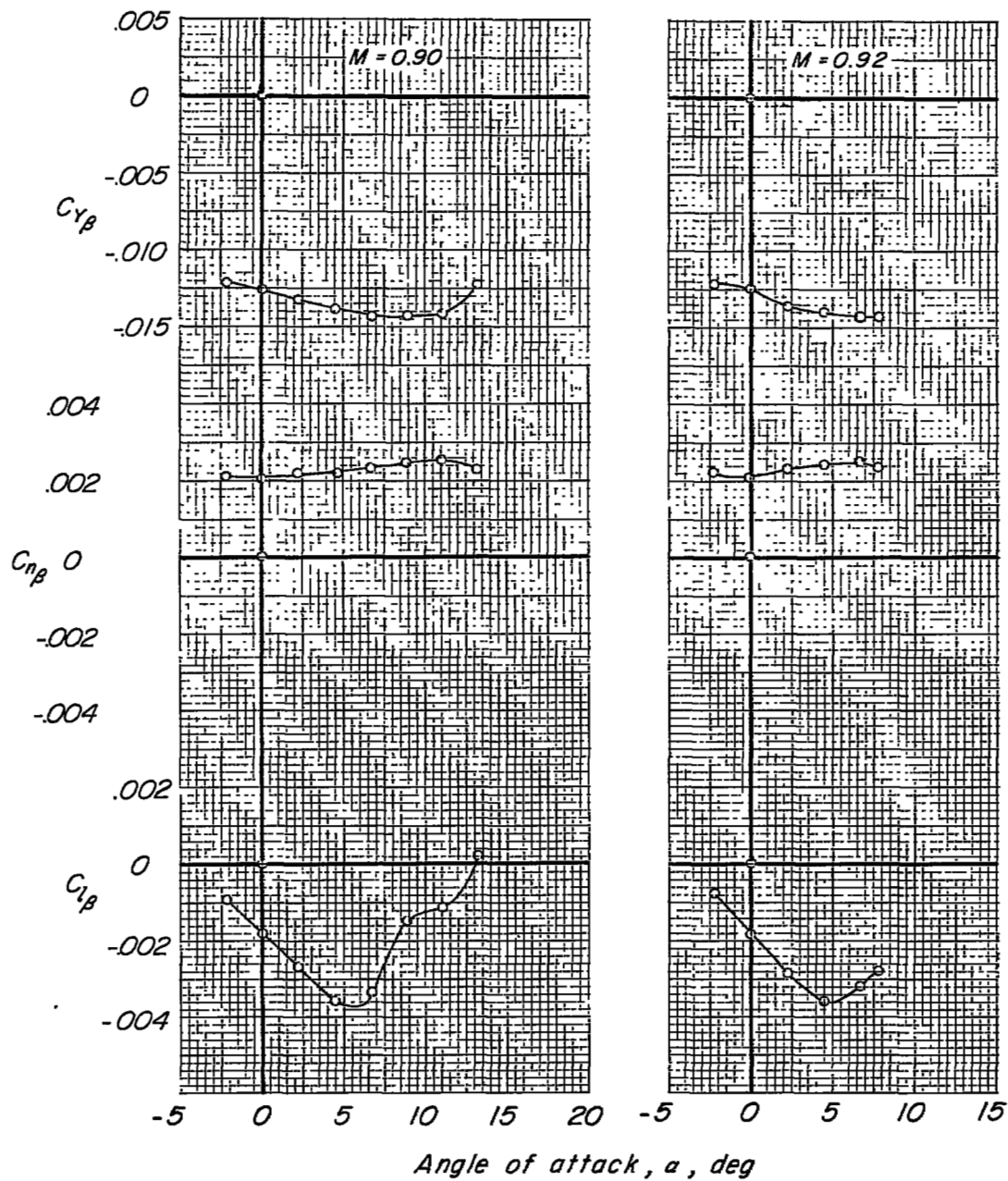


Figure 5.- Concluded.

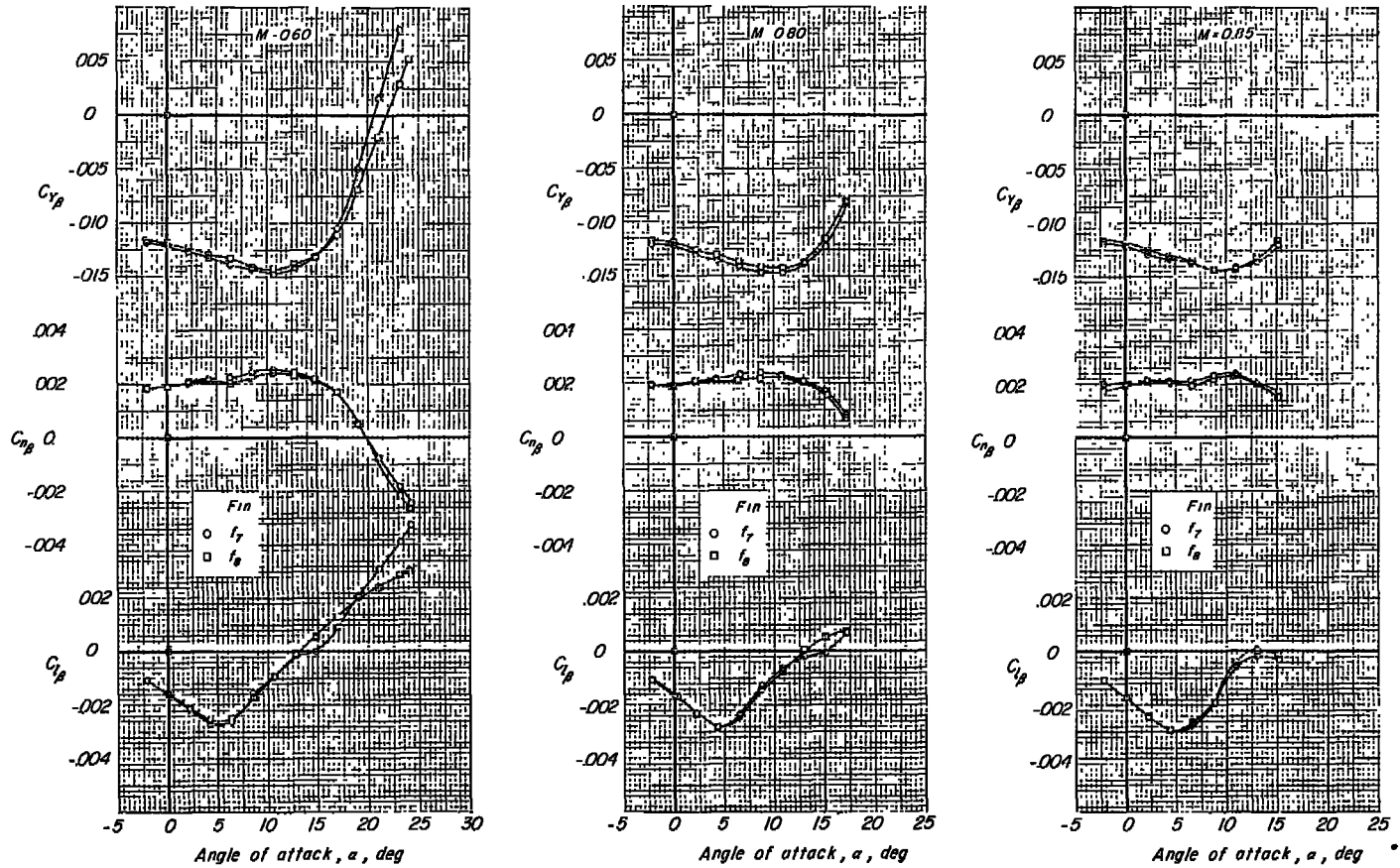


Figure 6.- Lateral stability derivatives of the complete model with the strakes, fin f_7 and f_8 .

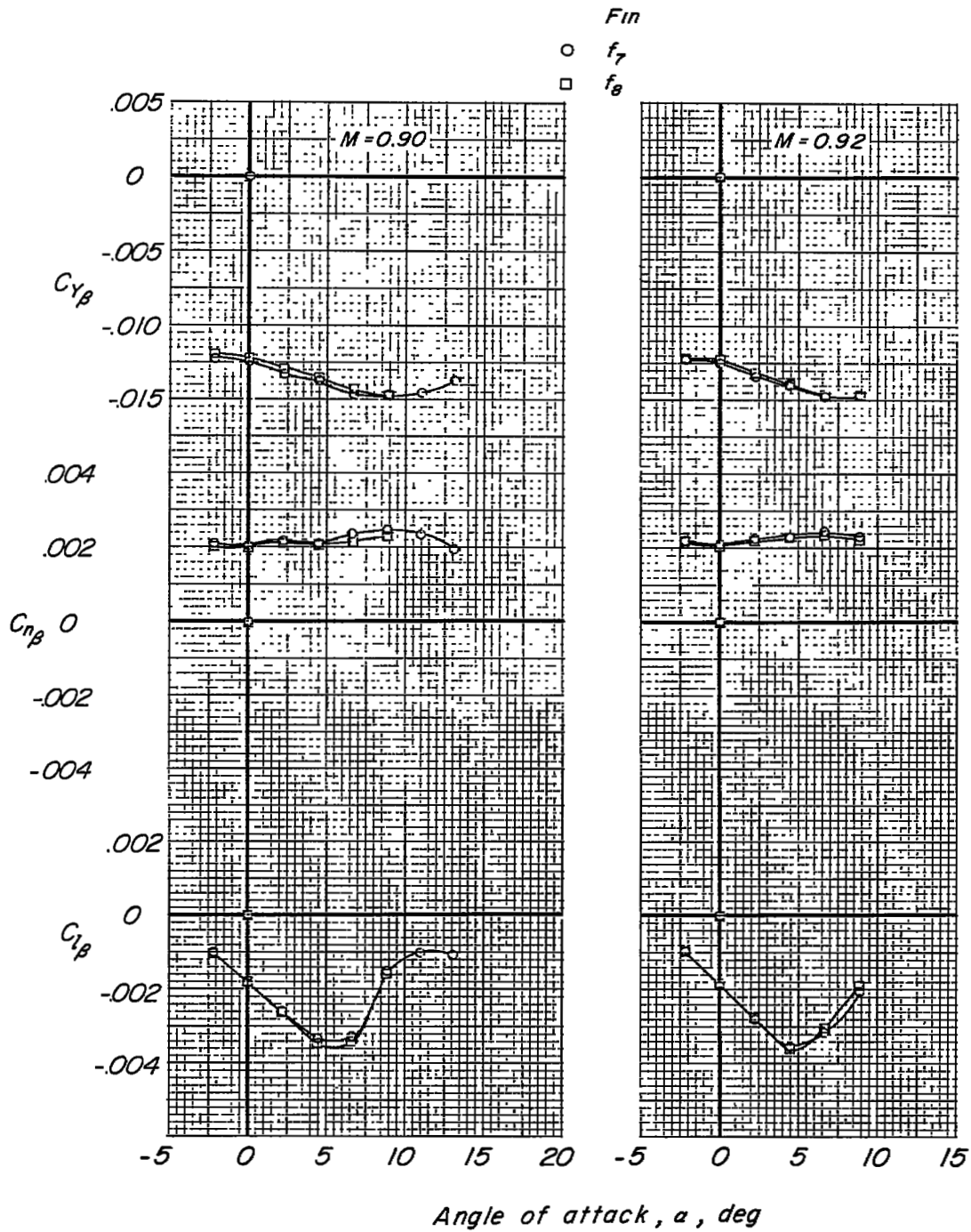


Figure 6.- Concluded.

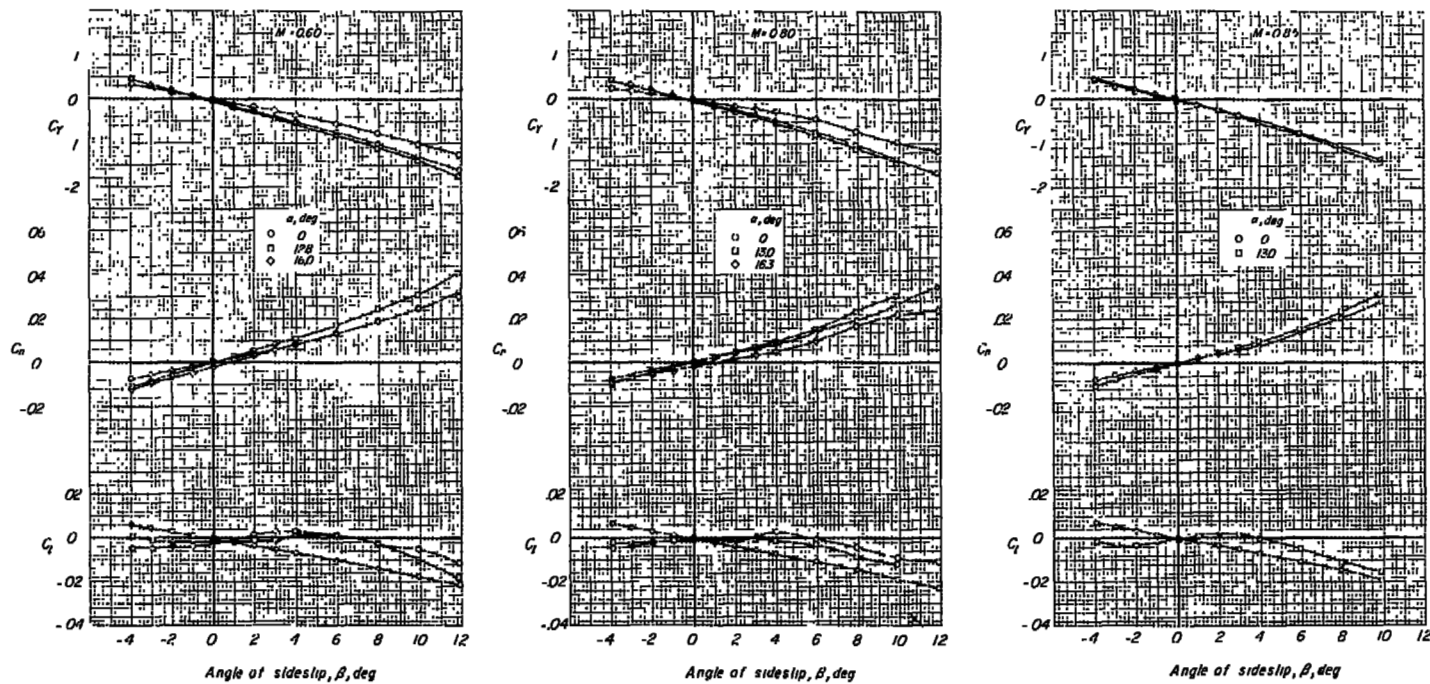


Figure 7.- Aerodynamic characteristics in sideslip of the complete model with the large strakes, fin f_6 .

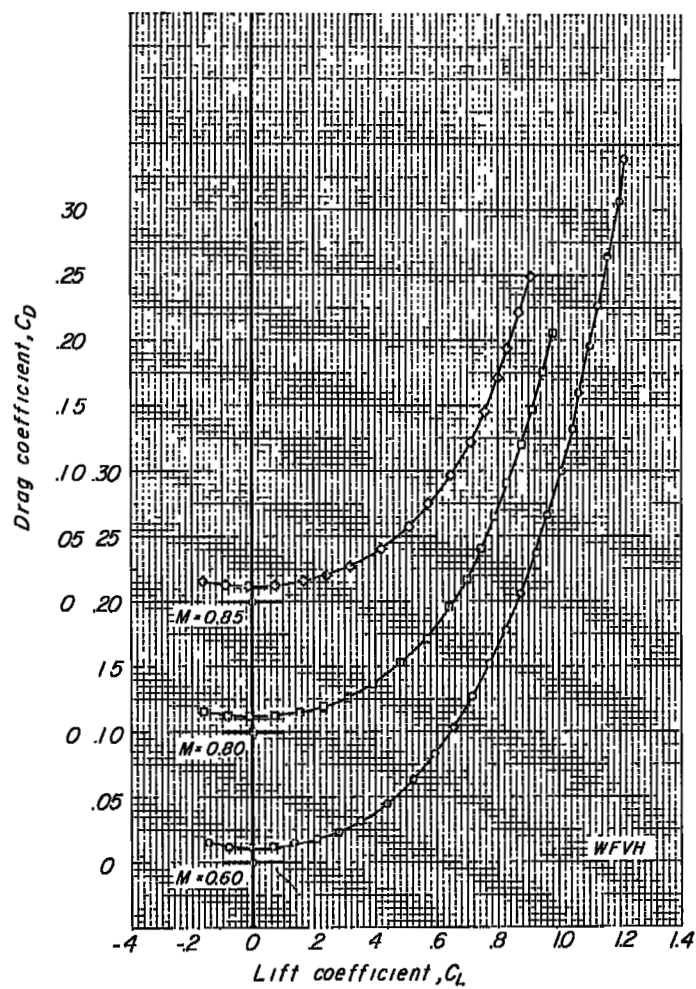
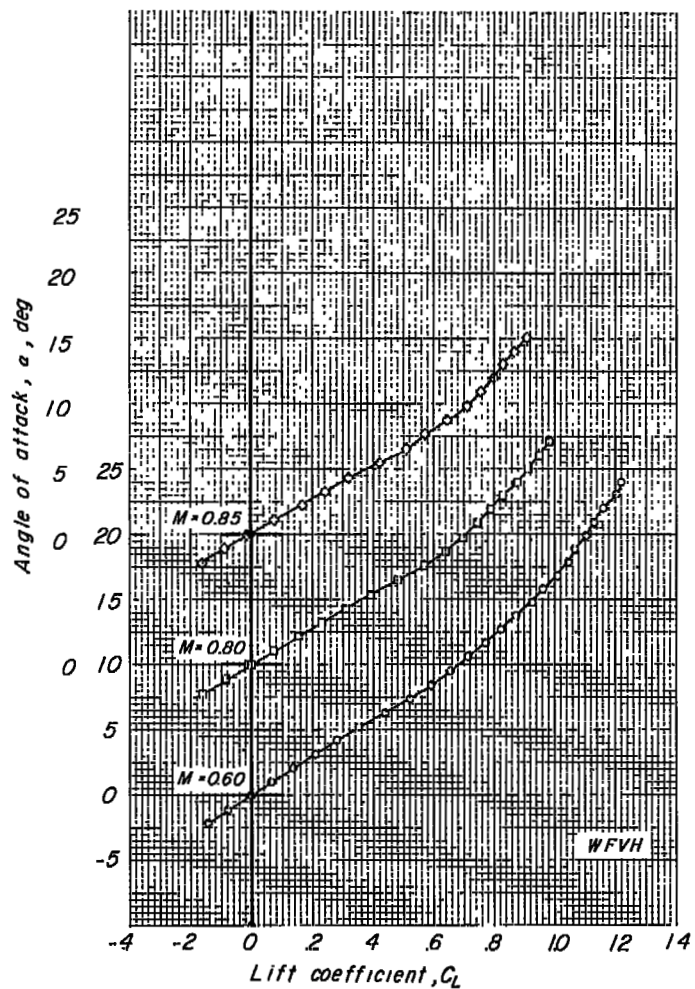


Figure 8.- Aerodynamic characteristics in pitch of the basic-model configuration.

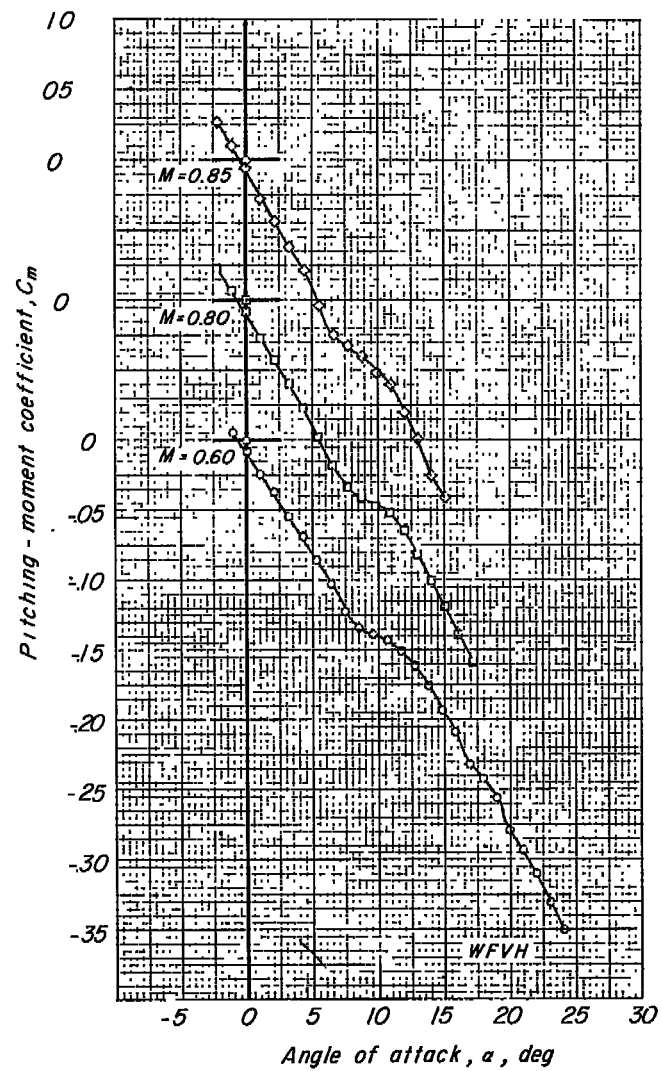
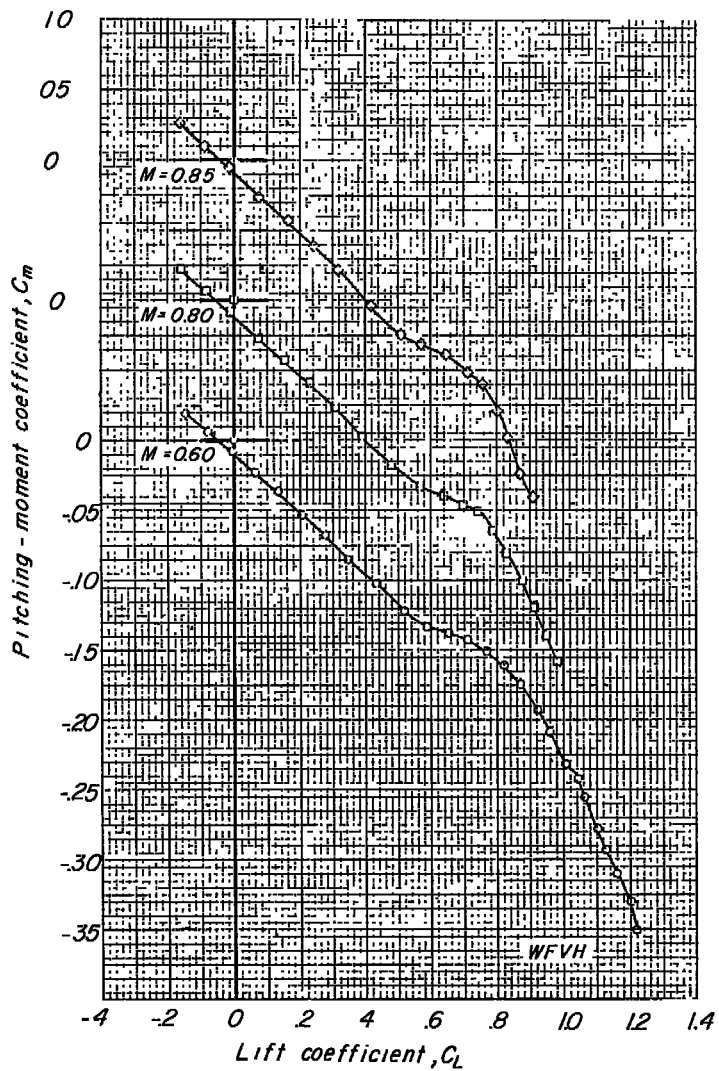


Figure 8.- Concluded.

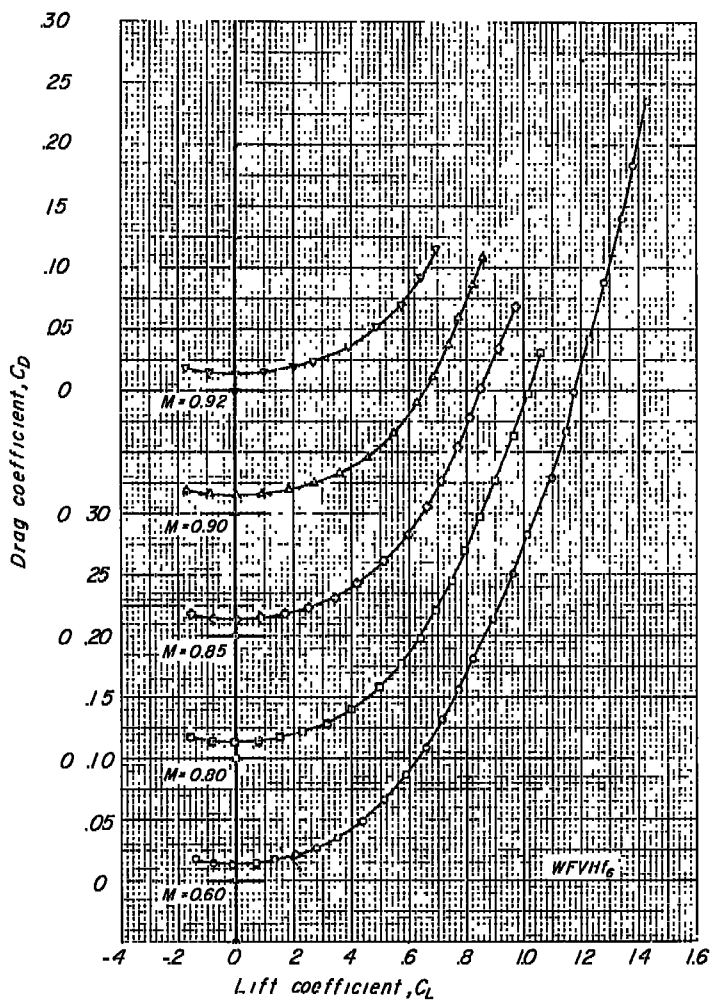
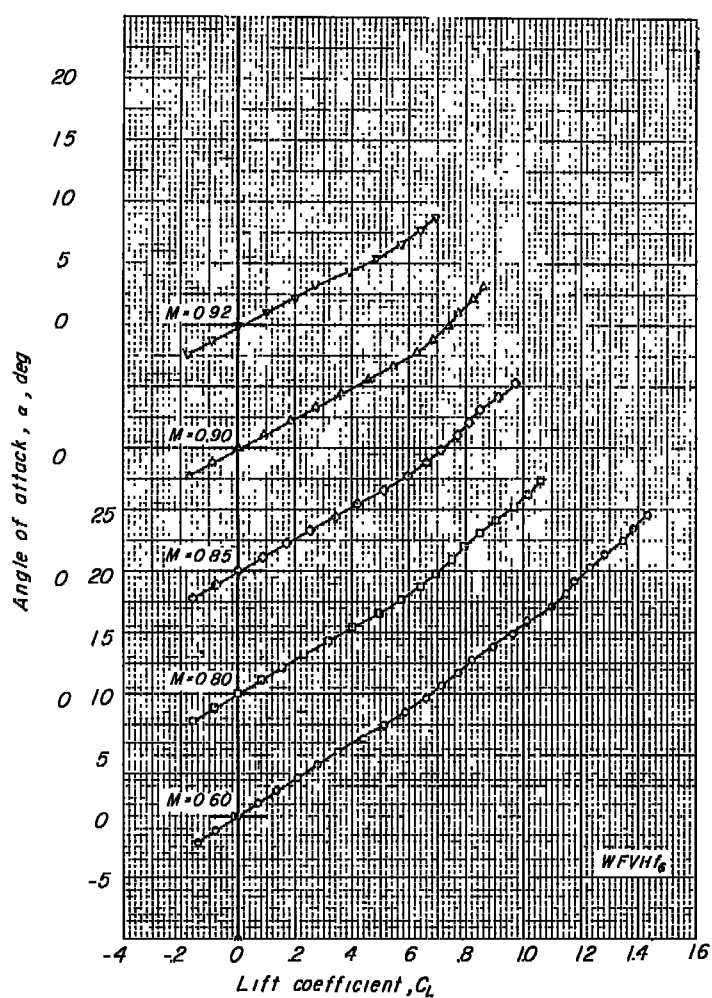


Figure 9.- Aerodynamic characteristics in pitch of the model with the large strakes, fin f₆.

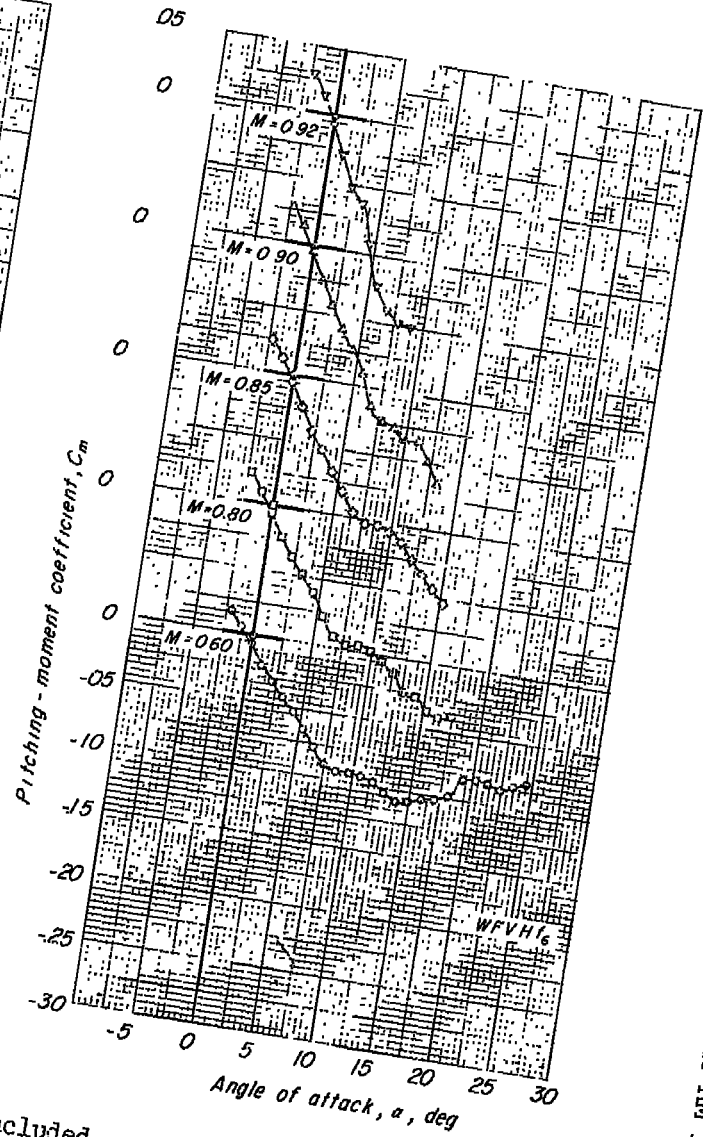
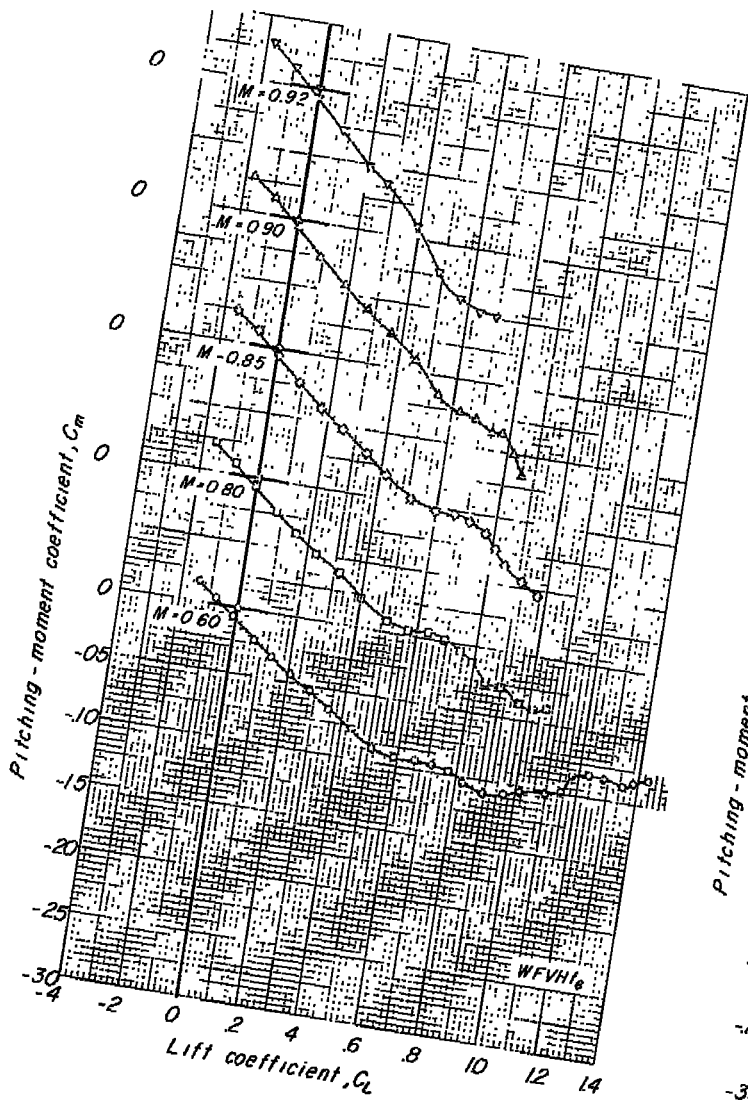


Figure 9.- Concluded.

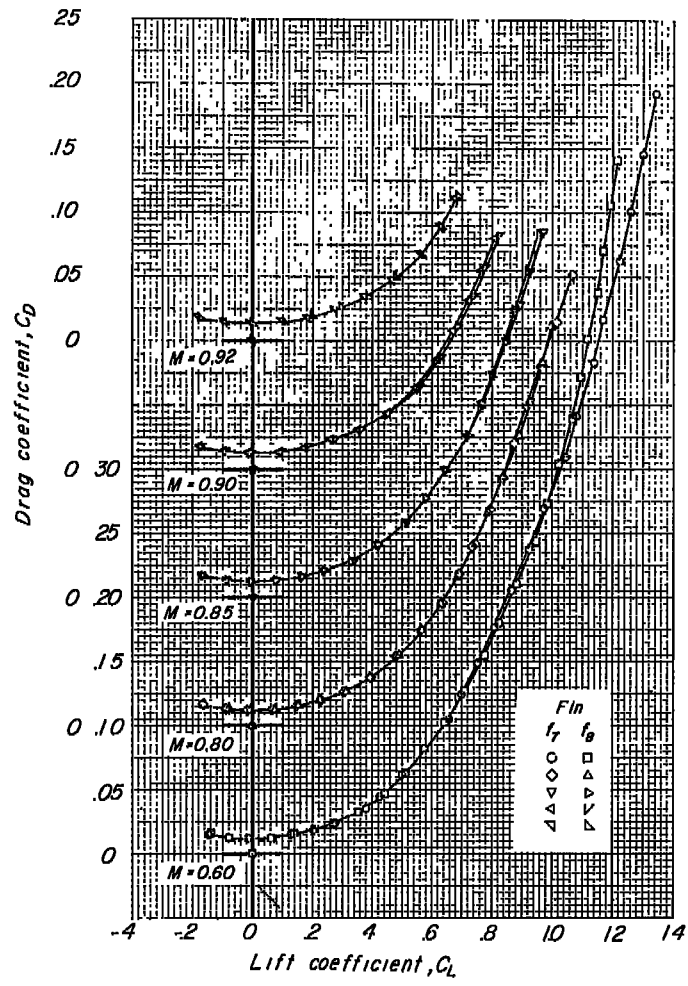
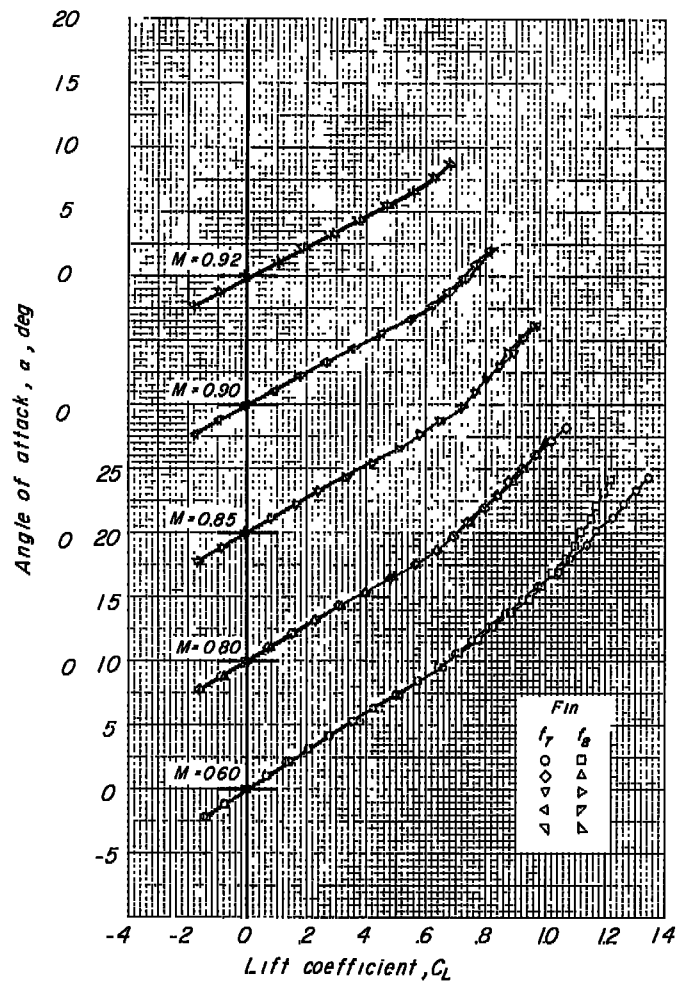


Figure 10.- Aerodynamic characteristics in pitch of the model with the strakes, fin f_7 and f_8 .

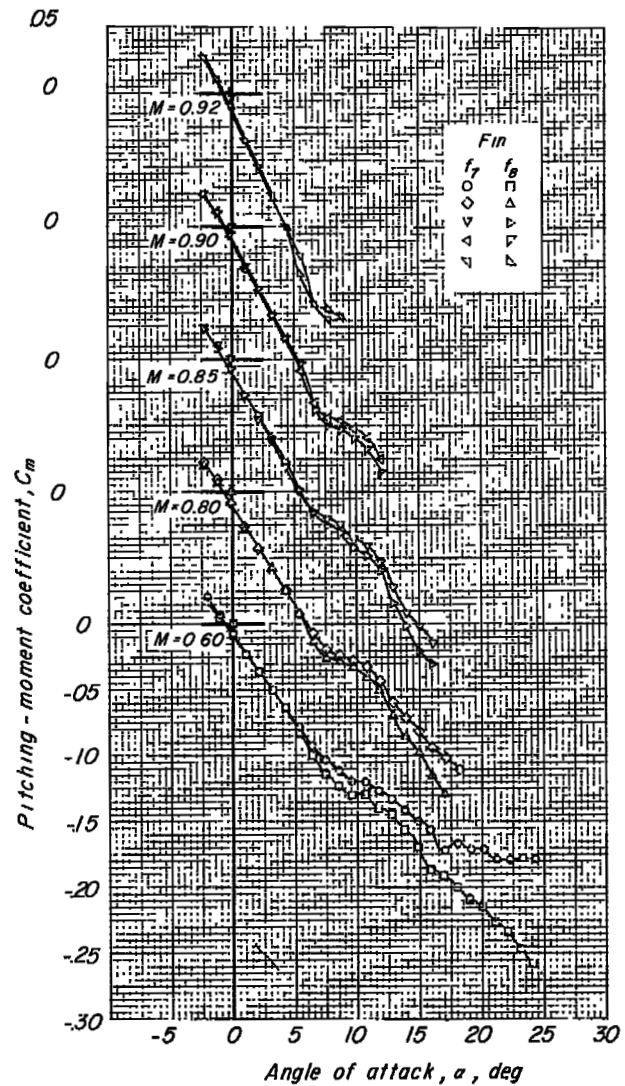
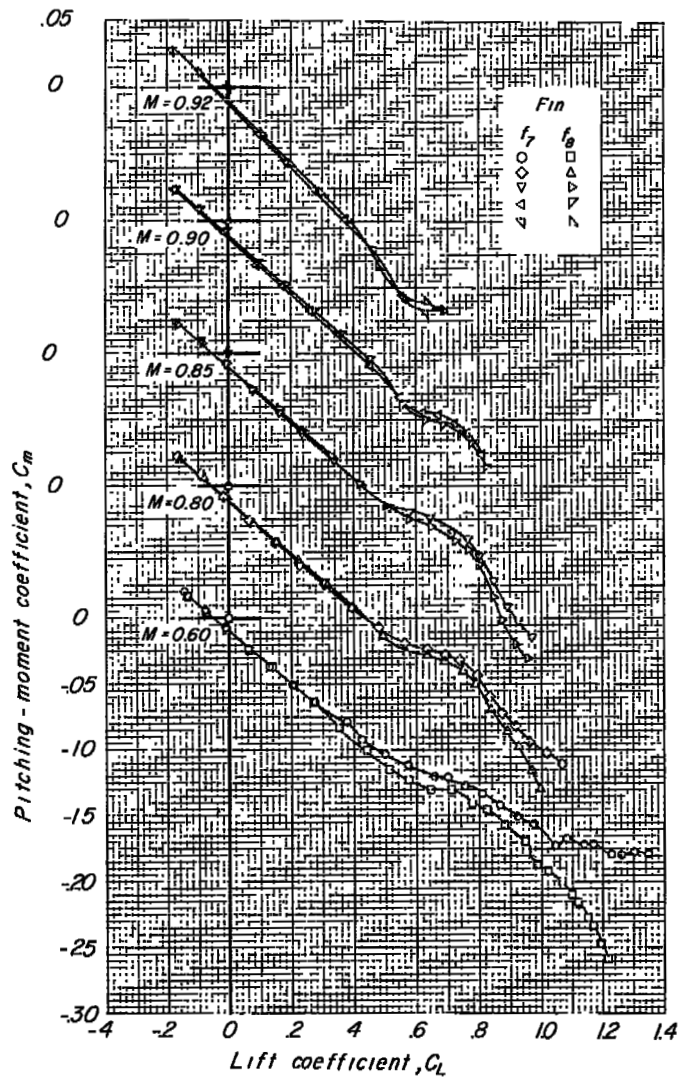


Figure 10.- Concluded.

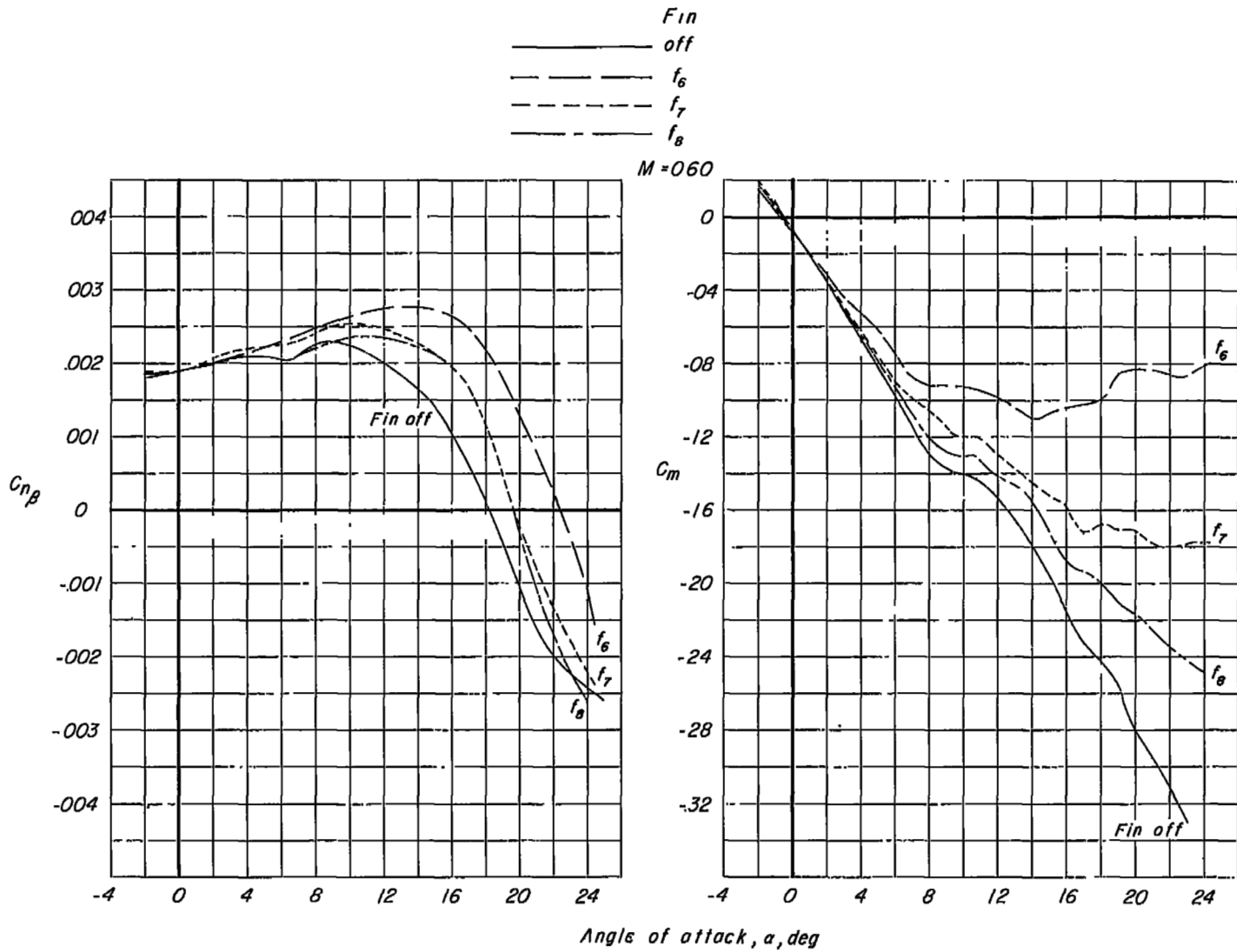
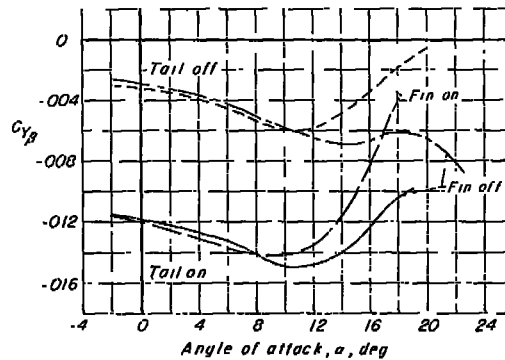
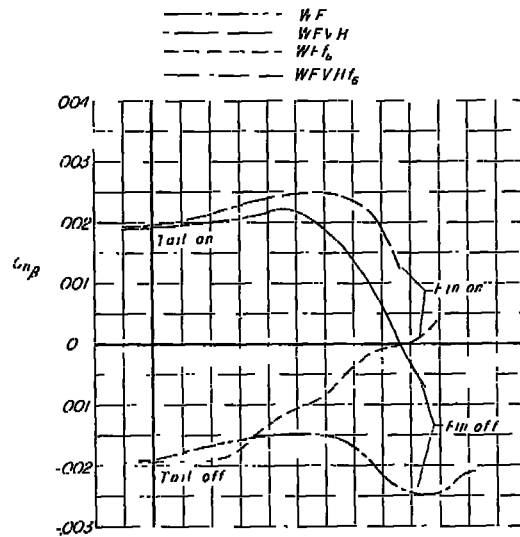
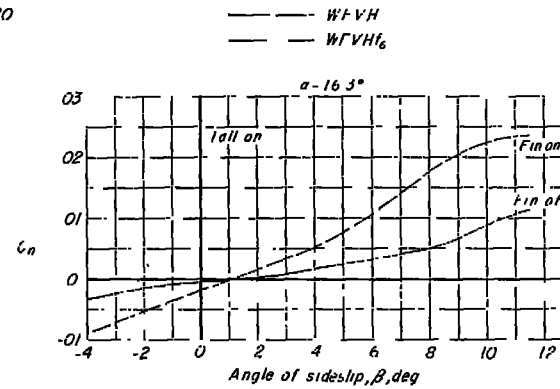
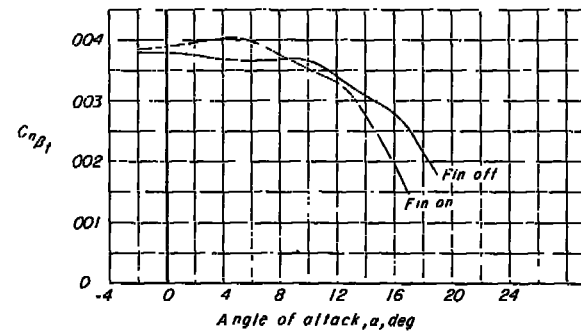


Figure 11.- Effects of the strakes on directional stability and pitching moments at $M = 0.60$.

(a) Effect on $C_{n\beta}$ and $C_{y\beta}$.

(b) Effect on yawing-moment characteristics in sideslip.



(c) Effect on tail contribution to directional stability.

Figure 12.- Summary of the effects of the large strakes, fin f_6 , on the directional stability characteristics of the model. $M = 0.80$.